Elsevier Editorial System(tm) for Nuclear Inst. and Methods in Physics Research, A
Manuscript Draft

Manuscript Number:

Title: Performance check of the CsI(Tl) calorimeter for the J-PARC E36 experiment by observing e^+ from muon decay

Article Type: Full length article

Section/Category: High Energy and Nuclear Physics Detectors

Keywords: Kaon decay; CsI(Tl) Calorimeter; Waveform Analysis

Corresponding Author: Dr. Hiroshi Ito,

Corresponding Author's Institution:

First Author: Hiroshi Ito

Order of Authors: Hiroshi Ito; Kate Horie, Ph D; Suguru Shimizu, Ph. D.; Sebastien Bianchin, Ph. D.; Chaden Djalali, Ph. D.; Bishoy Dongwi; David Gill, Ph. D.; Michael Hasinoff, Ph. D.; Yoichi Igarashi, Ph D; Jun Imazato, Ph. D.; N. Kalantarians, Ph. D.; Hideyuki Kawai, Ph. D.; Satoshi Kodama; Michael Kohl, Ph. D.; H. Lu, Ph D; O. Mineev; Makoto Tabata, Ph D; R. Tanuma; N. Yershov

Abstract: The J-PARC E36 experiment is searching for a lepton universality violation with a stopped kaon beam by measuring the ratio of the K^+ decay widths $¥Gamma(K_{e2})/¥Gamma(K_{¥mu2})=¥Gamma(K^+¥to e^+ ¥nu_e)/¥Gamma(K^+¥to ¥mu^+ ¥nu_¥mu)$. Since the radiative ${K^+¥to e^+ ¥nu_e ¥gamma}$ decays are backgrounds to be removed in this measurement, the radiated $¥gamma$ rays were detected in a CsI(Tl) calorimeter. The energy calibration for the 768 CsI(Tl) modules was performed using mono-chromatic $¥mu^+$s from the $K_{¥mu2}$ decays. The delayed e^+ signals from the muon decays were required in order to improve the S/N ratio of the $K_{¥mu2}$ peak by suppressing background events. In addition, a new energy calibration method of the CsI(Tl) calorimeter using stopped cosmic muons has been established.

Performance check of the CsI(Tl) calorimeter for the J-PARC E36 experiment by observing e^+ from muon decay

H. Ito[a,*], K. Horie[b], S. Shimizu[b,**], S. Bianchin[c], C. Djalali[d], B. Dongwi[e], D. Gill[c], M. Hasinoff[f], Y. Igarashi[g], J. Imazato[g], N. Kalantarians[h], H. Kawai[i], S. Kimura[i], A. Kobayashi[i], S. Kodama[i], M. Kohl[e], H. Lu[d], O. Mineev[j], M. Tabata[i], R. Tanuma[k], N. Yershov[j]

[a] *Department of Physics, Kobe University, Hyogo, 657-8501, Japan*
[b] *Department of Physics, Osaka University, Osaka, 560-0043, Japan*
[c] *TRIUMF, Vancouver, V6T 2A3, Canada*
[d] *Department of Physics and Astronomy, University of Iowa, Iowa City, IA 52242, USA*
[e] *Physics Department, Hampton University, VA 23668, USA*
[f] *Department of Physics and Astronomy, University of British Columbia, Vancouver, V6T, 1Z1, Canada*
[g] *High Energy Accelerator Research Organization (KEK), Tsukuba, 305-0801, Japan*
[h] *Virginia Union University, Natural Science Department, Richmond VA, 23220, USA*
[i] *Department of Physics, Chiba University, Chiba, 263-8522, Japan*
[j] *Institute for Nuclear Research, Moscow, 117312, Russia*
[k] *Department of Physics, Rikkyo University, Toshima, 171-8501, Japan*

Abstract

The J-PARC E36 experiment is searching for a lepton universality violation with a stopped kaon beam by measuring the ratio of the K^+ decay widths $\Gamma(K_{e2})/\Gamma(K_{\mu 2}) = \Gamma(K^+ \to e^+\nu_e)/\Gamma(K^+ \to \mu^+\nu_\mu)$. Since the radiative $K^+ \to e^+\nu_e\gamma$ decays are backgrounds to be removed in this measurement, the radiated γ rays were detected in a CsI(Tl) calorimeter. The energy calibration for the 768 CsI(Tl) modules was performed using mono-chromatic μ^+s from the $K_{\mu 2}$ decays. The delayed e^+ signals from the muon decays were required in order to improve the S/N ratio of the $K_{\mu 2}$ peak by suppressing background events. In addition, a new energy calibration method of the CsI(Tl) calorimeter using stopped cosmic muons has been established.

Keywords: Kaon decay, CsI(Tl) Calorimeter, Waveform Analysis

1. Introduction

The $K^+ \to l^+\nu_l$ decay channel is one of the best processes to search for a lepton universality violation [1–3]. The ratio of $K^+ \to e^+\nu_e$ (K_{e2}) and $K^+ \to \mu^+\nu_\mu$ ($K_{\mu 2}$) decay widths (R_K) can be very precisely calculated in the framework of the Standard Model (SM) under the assumption of μ–e universality as [4],

$$R_K^{\mathrm{SM}} = \frac{\Gamma(K_{e2})}{\Gamma(K_{\mu 2})} = (2.477 \pm 0.001) \times 10^{-5}. \quad (1)$$

In order to compare the experimental R_K value with the SM prediction, the internal bremsstrahlung process in radiative $K^+ \to e^+\nu_e\gamma$ ($K_{e2\gamma}^{\mathrm{IB}}$) and $K^+ \to \mu^+\nu_\mu\gamma$ ($K_{\mu 2\gamma}^{\mathrm{IB}}$) decay has to be included in the K_{e2} and $K_{\mu 2}$ samples. On the other hand, the structure dependent processes in radiative $K^+ \to e^+\nu_e\gamma$ ($K_{e2\gamma}^{\mathrm{SD}}$) and $K^+ \to \mu^+\nu_\mu\gamma$ ($K_{\mu 2\gamma}^{\mathrm{SD}}$) decays are backgrounds and should be removed in the analysis [3]. A deviation of the experimentally measured R_K from the SM value would lead to a μ–e universality violation and indicate the existence of New Physics beyond the SM.

The J-PARC E36 experiment aims to make a precise R_K measurement by adopting a stopped K^+ beam method [5, 6]. A separated 800 MeV/c K^+ beam was slowed down by a degrader and stopped in a position sensitive K^+ stopper. The momentum measurement of the charged particles was performed using a 12-sector ion-core superconducting toroidal spectrometer, as shown in Fig. 1. The ra-

*Corresponding author.
E-mail address: ito.hiroshi@crystal.kobe-u.ac.jp (H. Ito).
**Principal corresponding author.
E-mail address: suguru@phys.sci.osaka-u.ac.jp (S. Shimizu).

diated photon from the above radiative processes was measured by a CsI(Tl) calorimeter, an assembly of 768 CsI(Tl) crystals, which covers 75% of the total solid angle. The photon energy and hit position were obtained by summing the energy deposits and by determining the energy-weighted centroid, respectively. Since the SD component subtraction is one of the key issues in E36, the understanding of the CsI(Tl) performance is very important.

This paper is organized as follows. Details of the CsI(Tl) calorimeter and the analysis procedure are described in Section 2 and Section 3. In Section 4, a calibration method using the mono-chromatic μ^+s from the $K_{\mu 2}$ decays is explained. A new method of the CsI(Tl) energy calibration using stopped cosmic-ray muons is discussed in Section 5. The results obtained in the present studies are summarized in Section 6.

2. CsI(Tl) calorimeter

The CsI(Tl) calorimeter was originally constructed for the KEK-PS E246 experiment to search for a T-violating transverse muon polarization in $K^+ \to \pi^0 \mu^+ \nu_\mu$ decay [7–9]. There are 12 holes for outgoing charged particles and 2 holes for the beam entrance and exit. Each crystal had a coverage of 7.5° along both the polar and azimuthal directions. The length of the CsI(Tl) crystal was 25 cm which was enough to obtain sufficient energy resolution as well as avoid nuclear counter effects.

Since the CsI(Tl) calorimeter had to be operated under a relatively strong fringing field from the toroidal magnet where PMTs would be difficult to use, PIN photodiodes (PIN diodes) were employed to read out the scintillation light of the CsI(Tl) crystals. Each crystal with its associated PIN diode and pre-amplifier was assembled in an Al container of 0.1 mm thickness. A charge sensitive pre-amplifier with a time constant of 600 μs and a gain of 0.5 V/pC was attached directly to the PIN diode. The output signal from the pre-amplifier was fed to a shaping amplifier with 1 μs shaping time. The waveforms of the shaping amplifier outputs were recorded by VF48 flash ADC manufactured by the TRIUMF national laboratory [10]. The VF48 had a 10 μs time range and was operated with a 25 MHz external clock signal (1 TDC channel = 40 ns).

3. Waveform analysis

3.1. Waveform model

The γ-ray energy and timing can be determined by fitting the CsI(Tl) output signal using a dedicated waveform model function. A typical waveform from the CsI(Tl) calorimeter is shown in the Fig. 2 (a), as indicated by the black open circles. In the analysis, we adopted the following waveform formula as,

$$f(t) = \frac{A}{1-\exp\{-(t-\tau_0)/\lambda)\}} \cdot Freq\left(\frac{t-\tau_0-d}{\mu}\right) \cdot \left\{\frac{t-\tau_0}{\tau_1}\exp\left(1-\frac{t-\tau_0}{\tau_1}\right) + \varepsilon\frac{t-\tau_0}{\tau_2}\exp\left(1-\frac{t-\tau_0}{\tau_2}\right)\right\}, \quad (2)$$

where A is the amplitude of the pulse and τ_0 is the rise time. The λ,μ and τ_1,τ_2 parameters are time constants to express the rise and decay parts of the pulse, respectively. $d \sim 1$ μs is introduced for a timing adjustment and $\varepsilon \sim 0.06$ is the ratio of the two decay components. $Freq(x)$ is known as the frequency function given as

$$Freq(x) = \frac{1}{\sqrt{2}}\int_{\infty}^{x} exp(-t^2/2)dt. \quad (3)$$

Then, in order to determine these parameters, an equal-weighted χ^2 quantity is introduced as,

$$\chi^2 = \sum_{i=1}^{250}\left\{A_i - f(t_i)\right\}^2, \quad (4)$$

where A_i and t_i are the ADC value and time of the ith waveform points, respectively. The parameters in the model function were derived by minimizing the χ^2 values. The red line in Fig. 2 (a) is the fitting result using the above method, and the deviation of each data point (dh) is shown in fig. 2 (b). Typical χ^2 values are distributed in the region of 100−500 which is mainly due to the imperfect reproducibility of the CsI(Tl) output by the waveform model.

3.2. Pulse separation of pileup events

For the analysis of pileup events, the maximum dh value ($dh_{\max}$) was first determined in the entire region using a single-pulse fitting. The waveforms with $|dh_{\max}| > 10$ can be recognized as two or more than two pulse components. The deviation of the data points from the single-pulse fitting result for a typical pileup event is shown in Fig. 3 (b) as

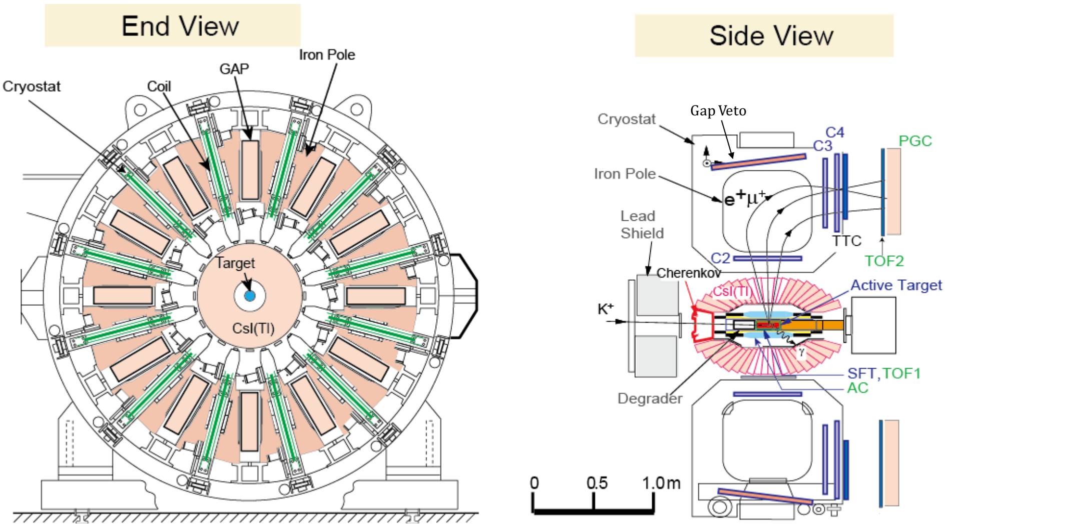

Fig. 1: Cross sectional end and side views of the setup for the J-PARC E36 experiment. The momentum vectors of charged particles and photons are determined by the toroidal spectrometer and the CsI(Tl) calorimeter, respectively.

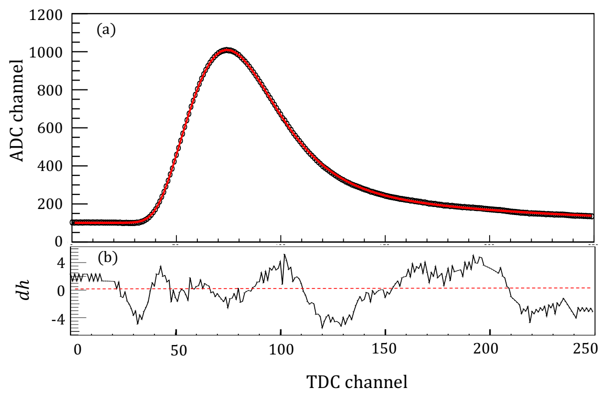

Fig. 2: (a) Typical waveform of the CsI(Tl) calorimeter signal. The open circles are the data and the red line is a fitting result of the waveform model. (b) The deviation of the data points from the fitting result.

the black line. These events were treated as pileup events, and multiple pulses in the fitting were taken into account. Then, the χ^2 value using a double-pluse waveform was again minimized by changing the fitting parameters. A typical pileup waveform is shown in Fig. 3 (a) as the black open circles. We can accept events as a double-pulse waveform with the conditions of (i) a waveform with $|dh_{\max}| < 10$, (ii) the time interval between the 1st and the 2nd signals is longer than 200 ns. The rejected events are treated as events with further multiple signals. The red and green solid lines in Fig. 3 (a) are the fitting results using the single-pulse and double-pulse fitting functions, respectively. The associated decomposed pulses are shown as the green (1st pulse) and blue (2nd pulse) dotted lines. The red line in Fig. 3 (b) shows the dh distribution assuming the double-pulse fittings, which indicates successful pulse separation using the double-pulse fitting.

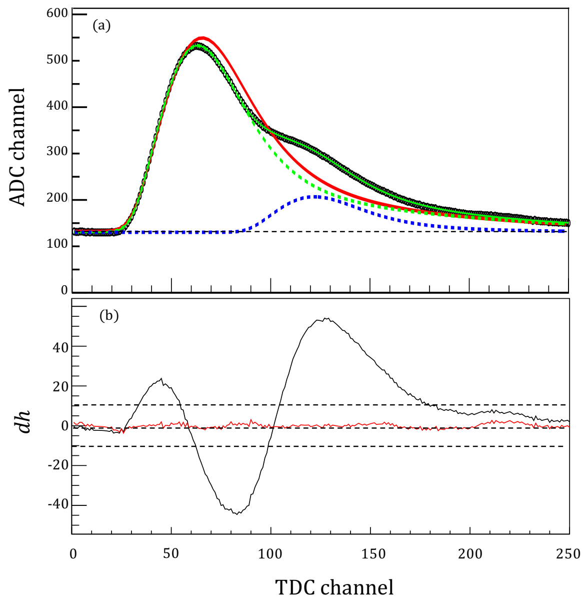

Fig. 3: (a) Typical pileup waveform of the CsI(Tl) calorimeter signal. The open circles are the data points. The red and green lines are the results adopting the single- and double-pulse fitting function. The green and blue dotted lines are the decomposed 1st and 2nd pulses. (b) The deviation of each data point from the fit curves. The black and red lines are the results using the single and double fitting.

4. CsI(Tl) calibration using $K_{\mu 2}$ decay events

4.1. Background reduction by observing the e^+ from μ^+ decay

The CsI(Tl) energy calibration was performed using mono-chromatic μ^+s from the $K_{\mu 2}$ decays at rest in the K^+ stopping target. The μ^+ kinetic energy was 152.5 MeV. These muons were stopped in the CsI(Tl) crystal and generated the delayed e^+ signal from the subsequent $\mu^+ \to e^+ \bar{\nu_\mu} \nu_e$ decay. The e^+ signal can be observed as the second pulse in the waveform analysis using the double-pulse fitting.

The $K_{\mu 2}$ events were selected by the following conditions: (I) the number of hit crystals was only one, (II) the first pulse time coincided with the K^+ decay, and (III) the waveform data was successfully analyzed as a double-pulse waveform.

The pulse height spectrum obtained by selecting events with the conditions of only (I) (II) are shown in Fig. 4 as the black histogram. On the other hand, the red histogram represents events selected with all the above conditions. It is clearly seen that background components below the $K_{\mu 2}$ peak are significantly removed by requiring the μ^+ decay in the CsI(Tl). Here, the backgrounds are considered to be mainly accidental events created by the beam particles.

Then, the signal to noise ratio (S/N) was calculated as,

$$\mathrm{S/N} = \frac{N(500 \le l < 800)}{N(l < 500,\ 800 \le l)}, \tag{5}$$

where l is the pulse height of the first pulse obtained by the fitting. The $K_{\mu 2}$ peak region and the background dominant region were separated as $N(500 \le l < 800)$ and $N(l < 500,\ 800 \le l)$, respectively. The S/N ratio was determined to be 0.42 for the events selected with the conditions of (1)(2). Next the μ^+ selection by requiring the double-pulse waveform was performed, and the S/N was obtained to be 4.42. Thus, we can conclude that the requirement of the μ^+ stop and decay in the CsI(Tl) is a very useful technique to reduce the backgrounds from the beam particles and make the CsI(Tl) energy calibration significantly more accurate.

4.2. CsI(Tl) performance check

For the CsI(Tl) energy calibration, the μ^+ energy loss in the target system should be added to the μ^+ energy observed by the CsI(Tl). The energy conversion factor, k, can be formulated as $k = (152.5 - E_t\ \mathrm{MeV})/l$, where E_t is the muon energy loss in the target. The μ^+ path length in the target was obtained by connecting the CsI(Tl) center of the μ^+ hit module and the K^+ vertex position determined by the target system. The typical k value was obtained to be 2.1–2.5 MeV^{-1}. Then, the μ^+ energy spectrum from the $K_{\mu 2}$ decay is obtained by taking into account the energy loss in the target as $E = kl + E_t$, as shown in Fig. 5. The red and blue spectra indicate the calibrated energy spectrum with and without the target energy correction, respectively. The target energy correction improved the energy resolution to σ=2.63% from 4.73%.

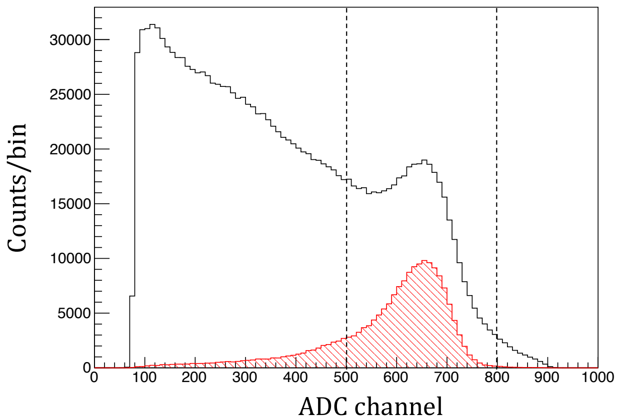

Fig. 4: Integrated pulse-height spectrum. The black spectrum shows the events selected with the conditions of (1)(2). The red shaded histogram shows the events selected with all the conditions. The region indicated by the two dotted lines is used to estimate the S/N ratio.

Also, the CsI(Tl) timing information was checked by requiring the e^+ signals to reduce the effects from accidental backgrounds. The 40 ns clock timing uncertainty of VF48 was corrected for by measuring the trigger signal in the same VF48 module. The timing resolution was determined to be 10.7 ± 0.1 ns (σ).

5. A new method of energy calibration using stopped comic-ray muons

It is possible to consider a new CsI(Tl) calibration method using stopped cosmic-ray muons with the subsequent e^+ emission in the CsI(Tl) calorimeter. This method is proposed to measure the e^+

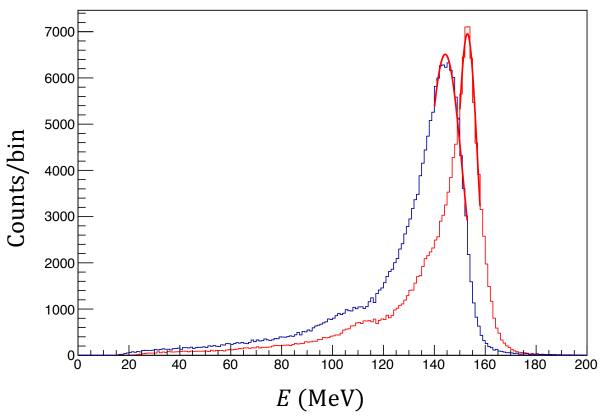

Fig. 5: The calibrated energy spectra obtained using the $K^+ \to \mu^+\nu_\mu$ decays. The red spectrum includes a correction for the energy loss in the target. The red lines are the fitting results assuming a Gaussian function.

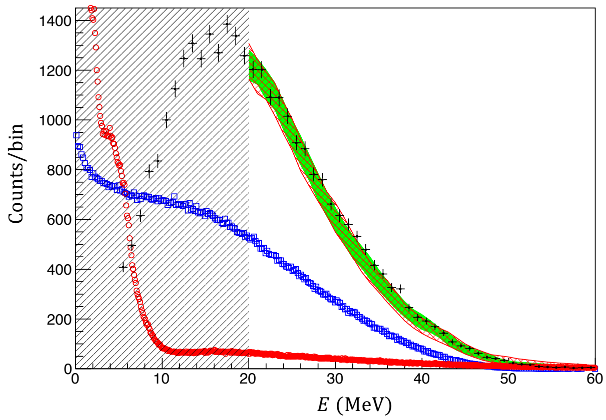

Fig. 6: Energy distributions of e^+ (e^-) from stopped cosmic muons. An electromagnetic gamma shower was taken into account in the simulation. The black hatched area is not used in the fitting because of the online threshold setting of 20 MeV.

energy spectrum for a rough CsI(Tl) energy calibration without the need for a radioactive beam. Since the maximum e^+ energy from the muon decay is 52.32 MeV, the energy calibration can be performed by measuring the e^+ energy after the cosmic-ray muon stops in the CsI(Tl) crystal. The cosmic muons stop homogeneously in the CsI(Tl), and we do not need to consider the specific structure of the CsI(Tl) calorimeter.

The energy distribution of the decomposed second pulse is shown in Fig. 6 as indicated by the black dots. Here the calibration parameters obtained from the $K_{\mu 2}$ decays were used. The blue squares and the red open circles are the calculated e^+ and e^- energy distribution, respectively, using a Monte Carlo simulation based on a GEANT4 code. Electromagnetic shower leakage from the muon stopped module was taken into account. The red cross-hatched area and the green filled area are e^+ and e^- energy distributions assuming the muon yield ratio $F_+/F_- = 1.1$ and 1.6, respectively [11–15]. The energy resolution of 2.63% (σ) obtained from the $K_{\mu 2}$ calibration result has been used.

In order to determinate the energy calibration parameters using stopped cosmic-ray muons, a common gain parameter relative to the energy coefficients obtained from the $K_{\mu 2}$ calibration results was introduced. The reduced χ^2_ν/NDF determined by comparing the experimental data with the simulation was calculated as a function of the the above relative gain coefficient, as shown in Fig. 7, where NDF is the number of degrees of freedom. The black dots and open squares correspond to the results obtained by assuming $F_+/F_- = 1.1$ and 1.6, respectively. It should be noted that the fitting region was chosen to be 20–60 MeV because the online energy threshold was set to 20 MeV. The black hatched area was not used for the fitting. Scattering of the χ^2_ν values is due to random smearing to account for the CsI(Tl) energy resolution The lines in the figure represent the fitting results using a parabolic function. As a result, the relative coefficients for $F_+/F_- = 1.1$ and 1.6 were determined to be 0.986 ± 0.033 and 1.001 ± 0.032, which indicates the gain coefficients obtained from the stopped cosmic muons are consistent with those from the $K_{\mu 2}$ events at the 3–4% level. Therefore, the experimental data were in good agreement with the above two simulation models, indicating a correct understanding of the e^+ and e^- behavior generated from the stopped muons.

The muon lifetime curve was also measured using the time interval between the 1st and 2nd pulses, as shown in Fig. 8 by the black dots. Fitting the data with an exponential function, the decay constant was determined to be 2.06 ± 0.03 μs ($\chi^2_\nu/NDF = 69.5/43$), as shown by the red line. The observed time constant is a little shorter than the theoretical value which indicates that most of the μ^- events are captured by CsI nuclei and do not contribute to the above lifetime measurement.

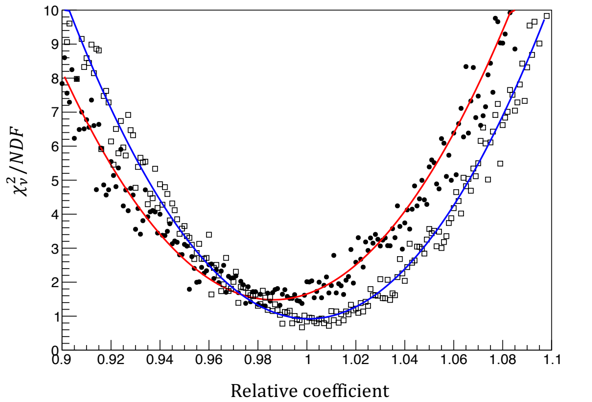

Fig. 7: Reduced χ^2_ν obtained by changing the relative gain coefficient. The black dots and open squares correspond to the results obtained by assuming $F_+/F_- = 1.1$ and 1.6, respectively. The lines in the figure represent the fitting results using a parabolic function. The gain coefficients obtained from the stopped cosmic muons are consistent with those from the $K_{\mu 2}$ events within 3–4%.

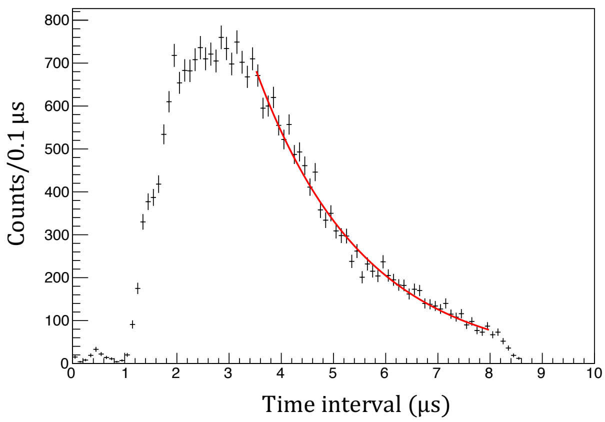

Fig. 8: Time interval between cosmic muons and the delayed e^+ (e^-) signals through the $\mu \to e\nu\bar{\nu}$ decays. The black dots and the red line are the data and fitting function, respectively.

6. Conclusion

A model function for the waveform analysis of CsI(Tl) calorimeter in the E36 experiment has been developed, and the information of the decomposed second pulses can be used for the event selection. The CsI(Tl) energy calibration was successfully performed by choosing the $K_{\mu 2}$ events and imposing the existence of the second pulses, and the S/N ratio was significantly improved. Then, the CsI(Tl) performance was carefully checked by studying the energy and timing resolutions.

A new energy calibration method using stopped cosmic muons is proposed. The energy and timing of the delayed e^+ (e^-) signals were determined by the decomposed second pulse in the double-pulse waveform analysis. The observed energy spectrum is consistent with the simulation calculation with an accuracy of 3–4%, indicating the establishment of a new calibration method without using any accelerator facilities.

Acknowledgement

This work was supported by a Grant-in-Aid for Scientific Research (C), No. 15K05113, from the Japan Society for the Promotion of Science (JSPS) in Japan and by NSERC and NRC (TRIUMF) in Canada. The authors thank H. Yamazaki for encouragement in executing this work. We would like to thank the J-PARC staff for the excellent beam delivery during our experimental beamtime.

References

[1] G. Lamanna et al., Nucl. Part. Phys. Proc. **273-275** (2016) 1671.

[2] C.Lazzeroni et al., Phys. Lett. B **719** (2013) 326.

[3] F. Ambrosino et al., Europ. Phys. J. C **64** (2009) 627.

[4] V. Cirigliano and I. Rosell, Phys. Rev. Lett. **99**, 231801 (2007).

[5] S. Shimizu, et al., Proposal for J-PARC 50 GeV Proton Synchrotron, P36 Jun 2010.

[6] S. Strauch et al., Proc. Scie., PoS(KAON13)014, 2013.

[7] M. Abe et al., Phys. Rev. D **73,** 072005 (2006).

[8] J.A.Macdonald et al., Nucl. Instrum. Methods A **506** (2003) 60.

[9] D.V. Dementyev et al., Nucl. Instrum. Methods A **440** (2000) 151.

[10] Y. Igarashi and M. Saito, in: IEEE 2012 Nuclear Science Symposium and Medical Imaging Conference Record (NSS/MIC).

[11] S. Haino et al., Phys. Lett. B **594**, 35 (2004).

[12] P. Archard et al., Phys. Lett. B **598**, 15 (2004).

[13] P. Adamson et al., Phys. Rev. D **76**, 052003 (2007).

[14] V. Khachatryan et al., Phys. Lett. B **692**, 83 (2010).

[15] N. Agafonova et al., Eur. Phys. J. C **67**, 25 (2010).

Figure1

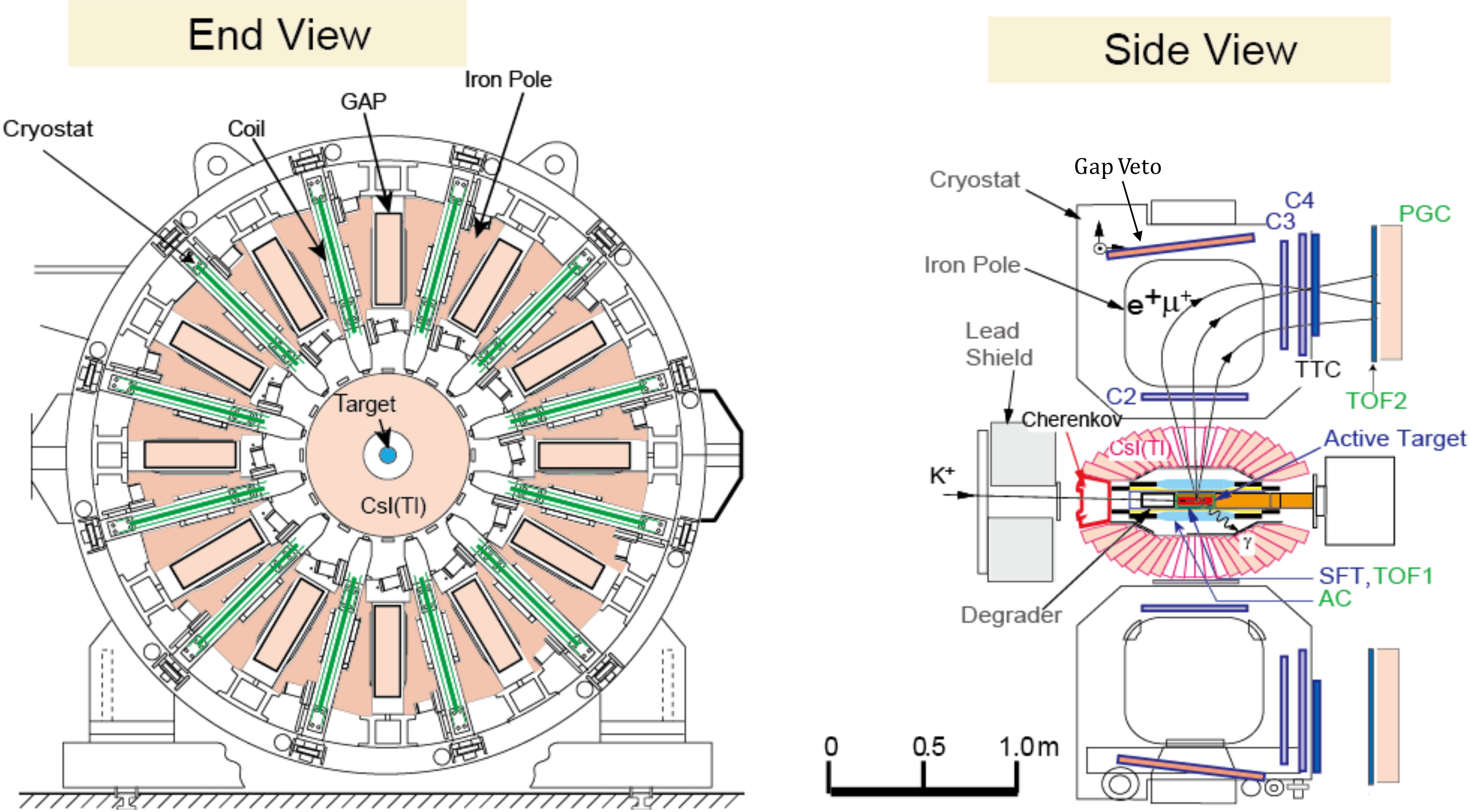
End View
Iron Pole
GAP
Cryostat
Coil
Target
CsI(Tl)
Side View
Gap Veto
Cryostat
C4
C3
PGC
Iron Pole
e+μ+
Lead
Shield
TTC
C2
TOF2
Cherenkov
Active Target
CsI(Tl)
K+
γ
SFT, TOF1
AC
Degrader
0
0.5
1.0m

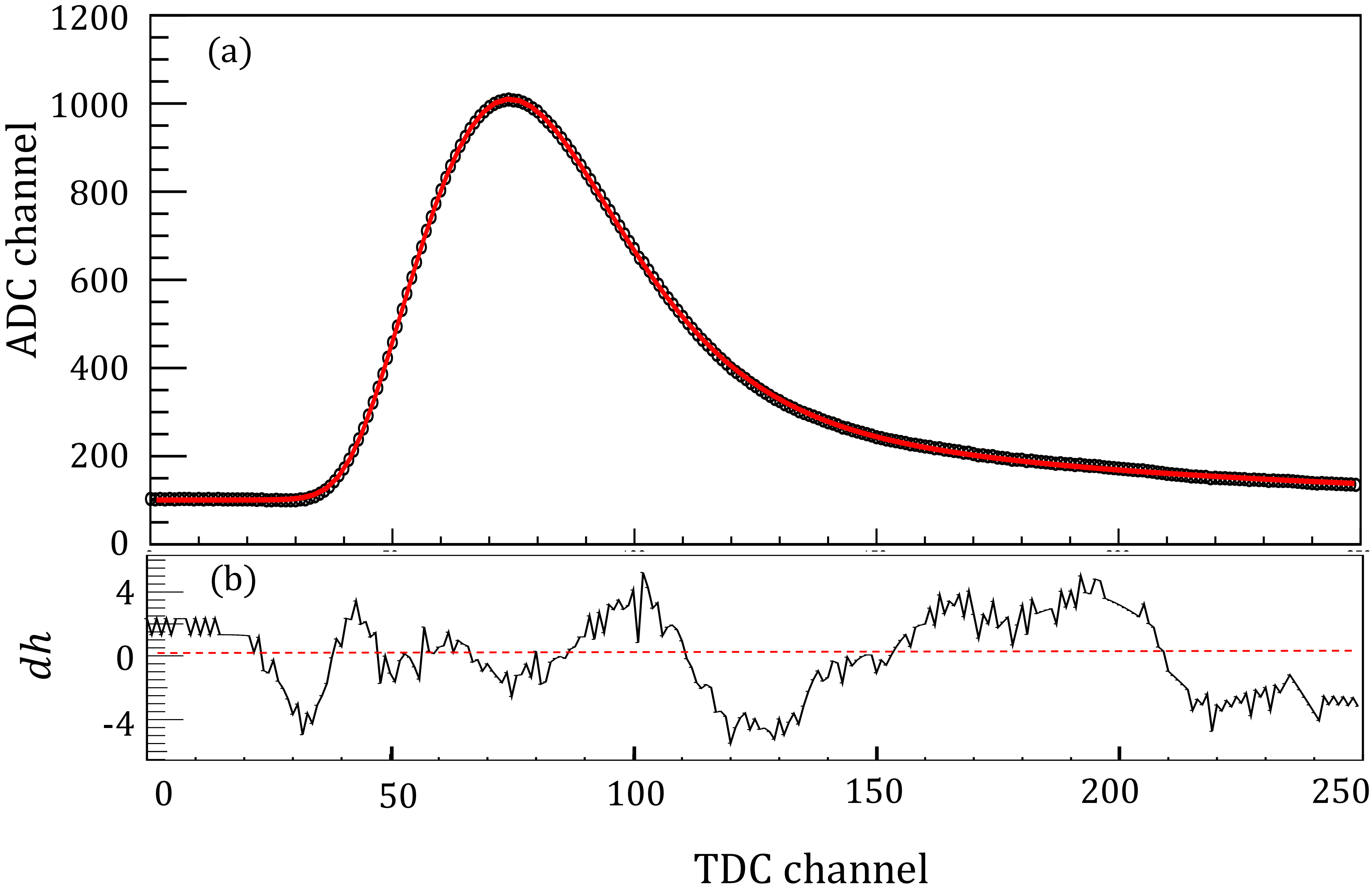

1200
1000
800
600
400
200
0
ADC channel
(a)
(b)
4
0
-4
dh
0
50
100
150
200
250
TDC channel

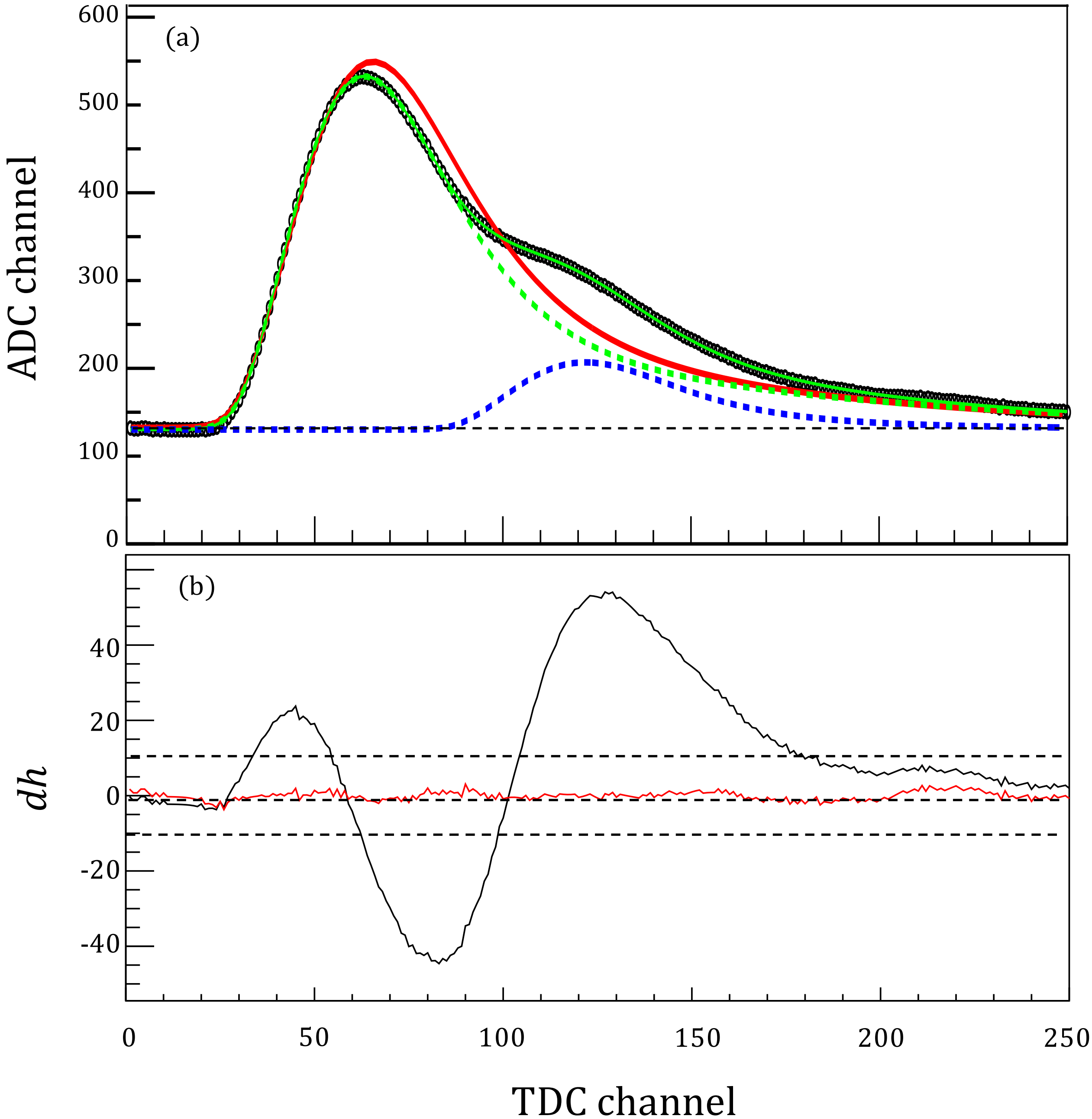

(a)
ADC channel
600
500
400
300
200
100
0
(b)
dh
40
20
0
-20
-40
0
50
100
150
200
250
TDC channel

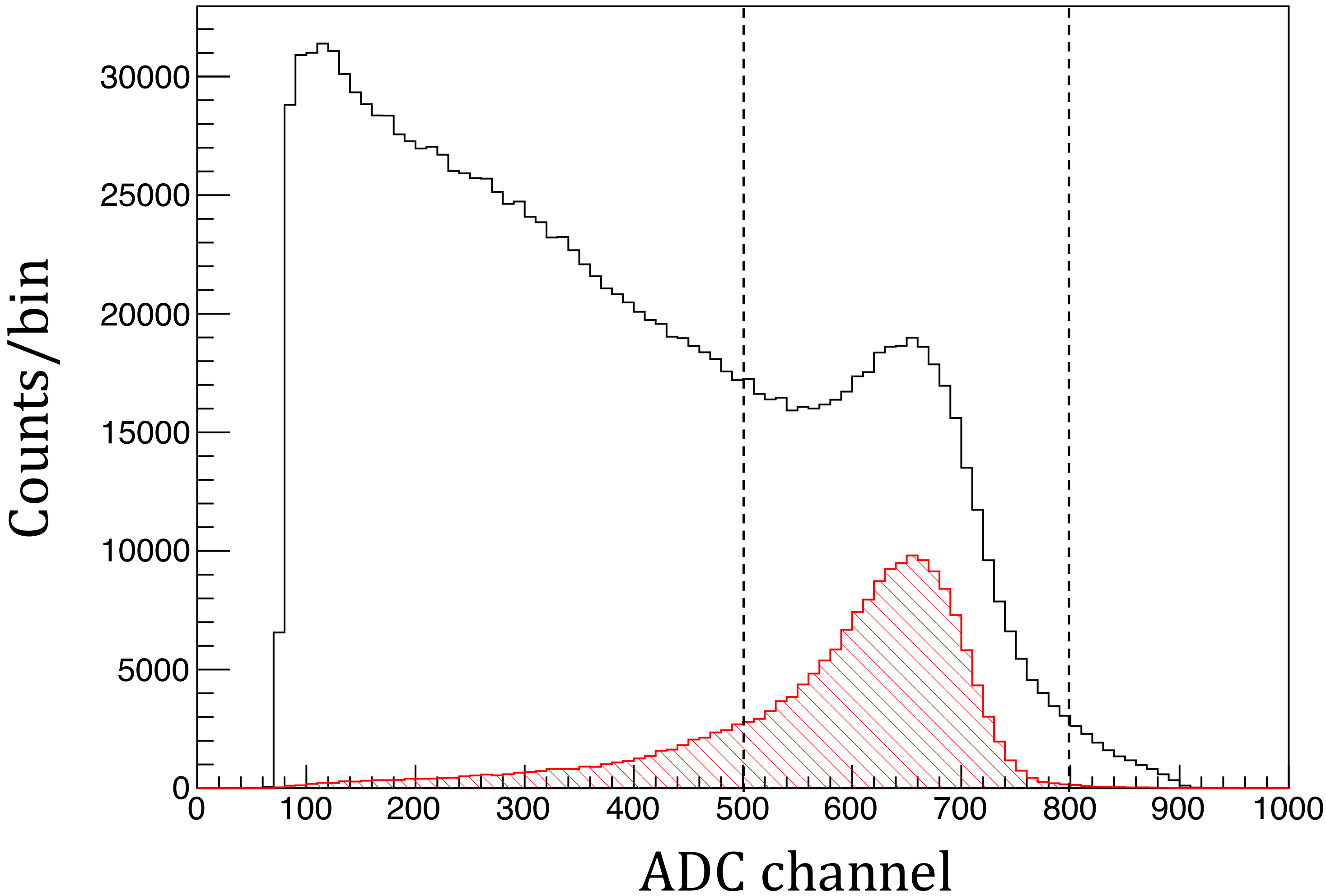

Counts/bin
30000
25000
20000
15000
10000
5000
0
0
100
200
300
400
500
600
700
800
900
1000
ADC channel

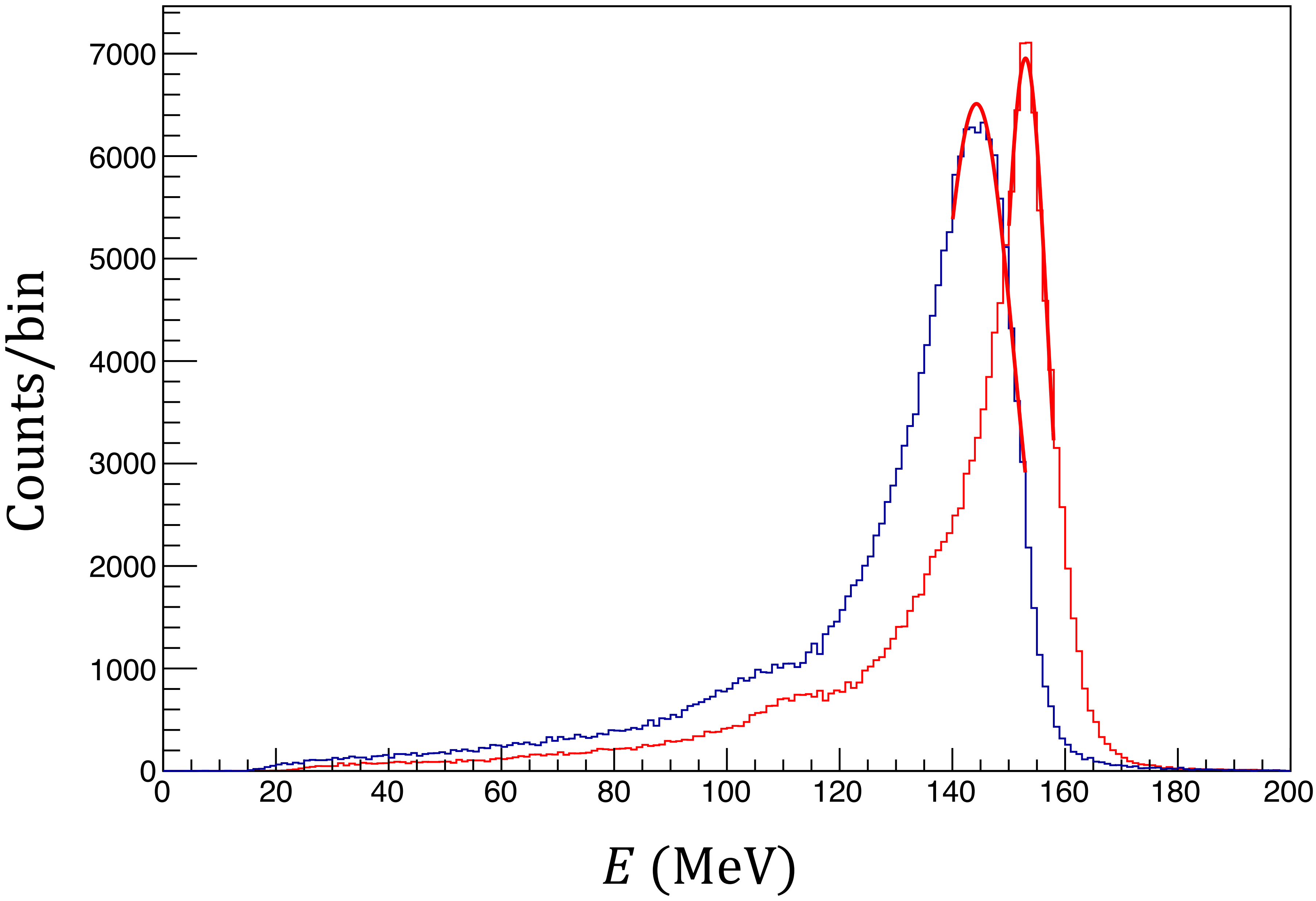

Counts/bin
0
1000
2000
3000
4000
5000
6000
7000
0
20
40
60
80
100
120
140
160
180
200
E (MeV)

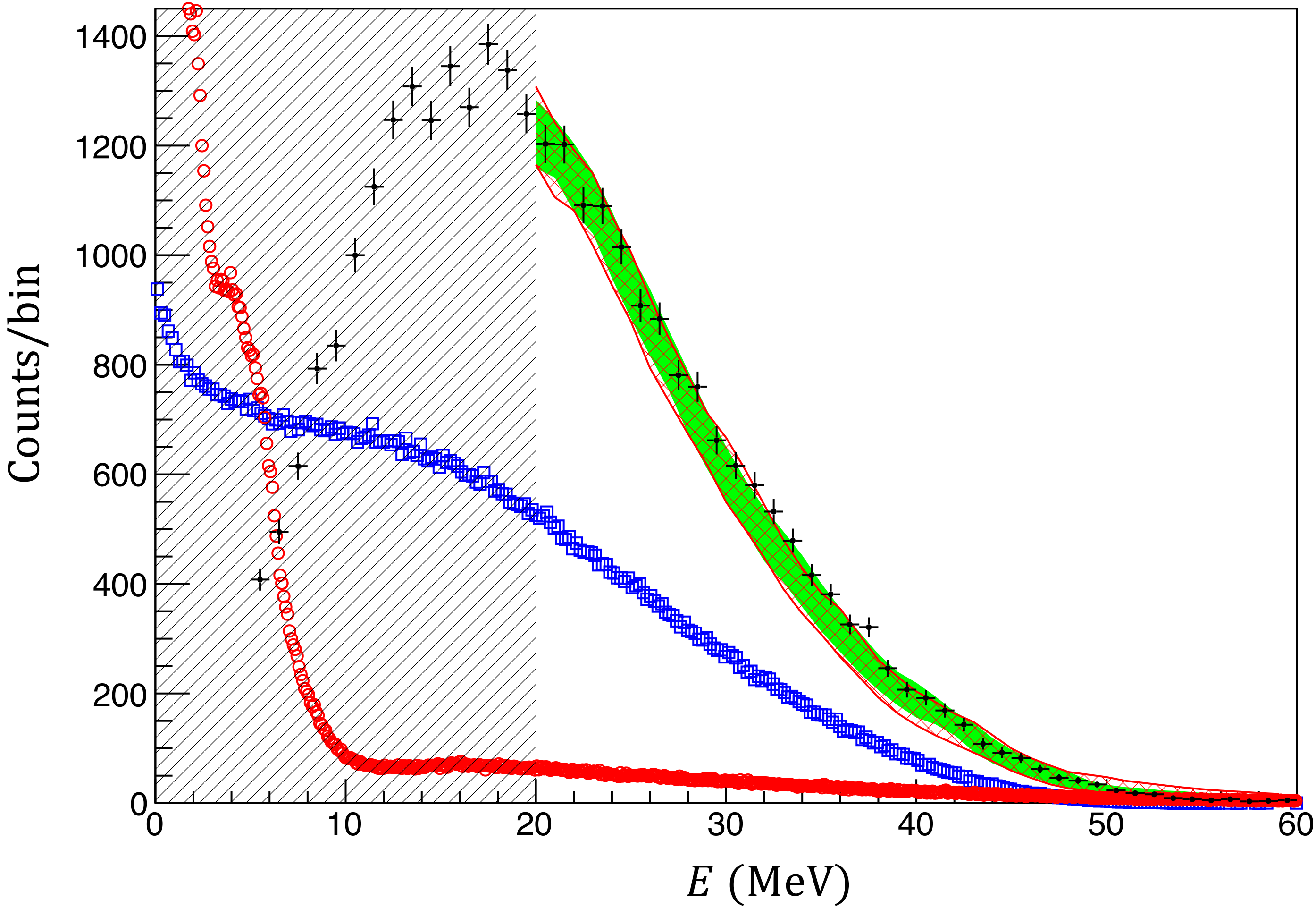
Counts/bin
0
200
400
600
800
1000
1200
1400
0
10
20
30
40
50
60
E (MeV)

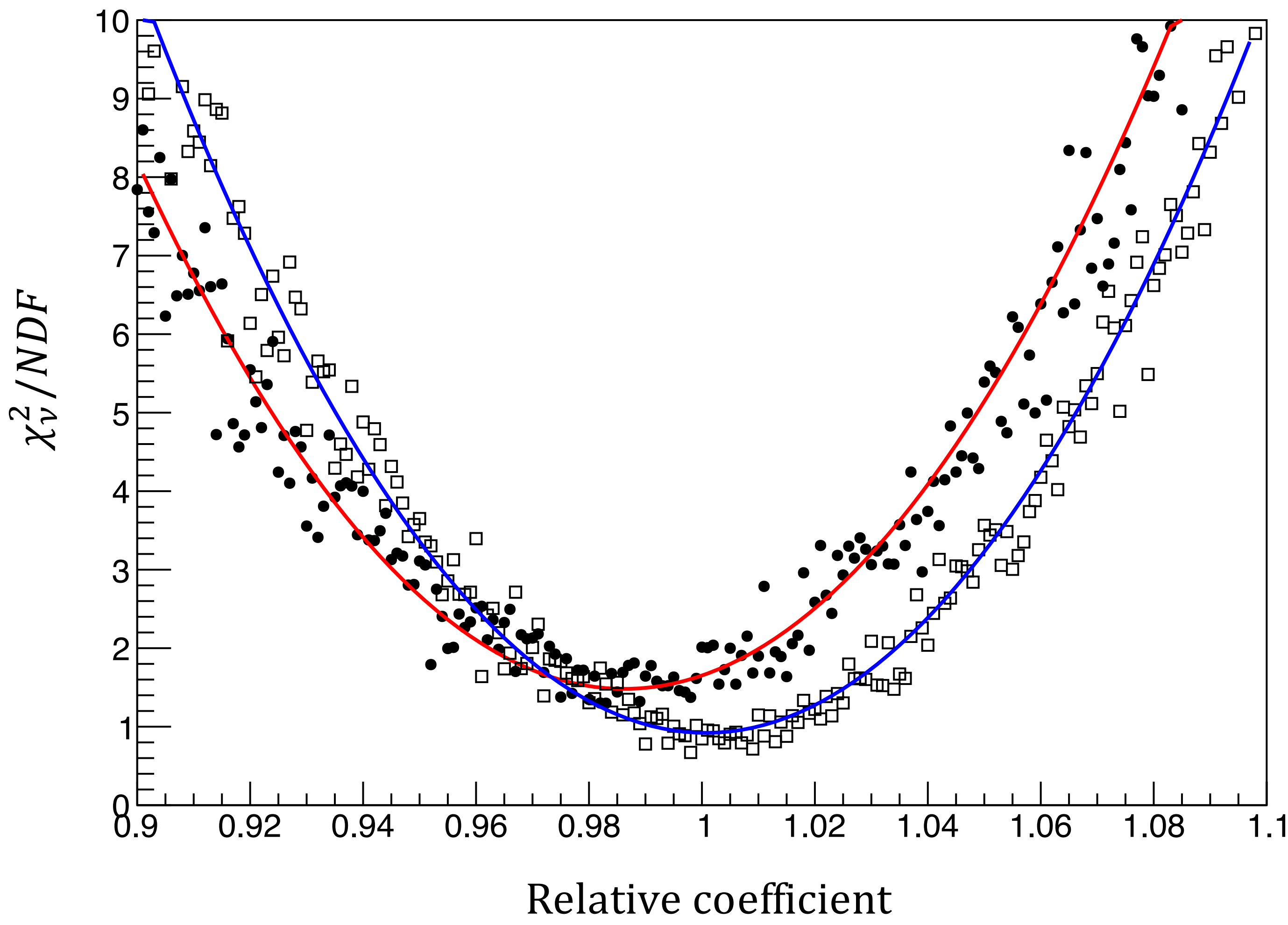

χ_ν^2/NDF
10
9
8
7
6
5
4
3
2
1
0
0.9
0.92
0.94
0.96
0.98
1
1.02
1.04
1.06
1.08
1.1
Relative coefficient

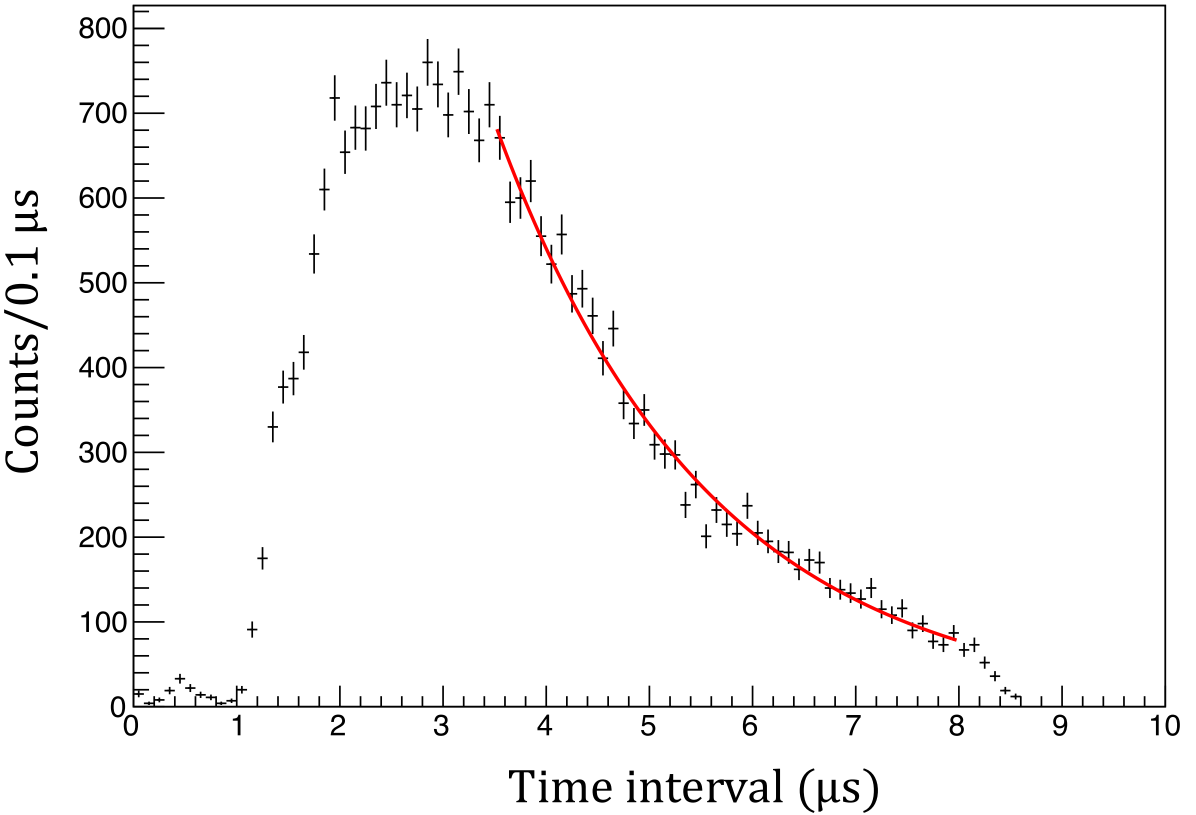

Counts/0.1 μs
800
700
600
500
400
300
200
100
0
0
1
2
3
4
5
6
7
8
9
10
Time interval (μs)